

# Anomalous quartic $ZZ\gamma\gamma$ couplings at the CLIC

M. Köksal\*

*Department of Physics, Cumhuriyet University, 58140, Sivas, Turkey*

## Abstract

We study the anomalous quartic  $ZZ\gamma\gamma$  couplings through the processes  $e^+e^- \rightarrow ZZ\gamma$ ,  $e^+e^- \rightarrow e^+\gamma^*e^- \rightarrow e^+ZZe^-$ , and  $e^+e^- \rightarrow e^+\gamma^*\gamma^*e^- \rightarrow e^+ZZe^-$  at the CLIC. We perform a model independent analysis defining genuine quartic gauge couplings and find 95% confidence level bounds on these couplings. The best bounds on the anomalous  $ZZ\gamma\gamma$  couplings between three processes is obtained through the process  $e^+e^- \rightarrow ZZ\gamma$  at a center of mass energy of 3 TeV and integrated luminosity of  $590 \text{ fb}^{-1}$ . We have shown that the obtained bounds on both anomalous coupling parameters are at the order of  $10^{-8} \text{ GeV}^{-2}$ , which significantly improves the current bounds.

---

\*mkoksal@cumhuriyet.edu.tr

## I. INTRODUCTION

In the context of the standard model (SM), self-interactions of gauge bosons are exactly determined by  $SU(2)_L \otimes U(1)_Y$  gauge symmetry. For this reason, the research of these couplings plays an important role in finding out the gauge structure of the SM. Any deviation of the triple and quartic couplings of the gauge bosons from the SM expectations would indicate the existence of possible new physics which can be stated in a model independent analysis by means of the effective Lagrangian approach. Such an approach is described by high-dimensional operators which give rise to genuine quartic gauge couplings. These effective operators also do not cause new trilinear vertices. Therefore, genuine quartic gauge couplings can be independently studied from trilinear couplings. The charge and parity conserving dimension 6 effective Lagrangian includes at least two photons that induce the  $ZZ\gamma\gamma$  vertex imposing the global custodial  $SU(2)$  and local  $U(1)$  symmetry defined by the operators [1, 2]

$$L = L_0 + L_c, \quad (1)$$

$$L_0 = \frac{-\pi\alpha}{4} \frac{a_0}{\Lambda^2} F_{\mu\nu} F^{\mu\nu} W_\alpha^{(i)} W^{(i)\alpha}, \quad (2)$$

$$L_c = \frac{-\pi\alpha}{4} \frac{a_c}{\Lambda^2} F_{\mu\alpha} F^{\mu\beta} W^{(i)\alpha} W_\beta^{(i)} \quad (3)$$

where  $W^{(i)}$  is  $SU(2)_{weak}$  triplet,  $F_{\mu\nu}$  is the photon field strength tensor, and  $a_0$  and  $a_c$  are the dimensionless anomalous coupling constants.

The  $Z^\mu Z^\nu \gamma^\alpha \gamma^\beta$  vertex functions produced by dimension 6 effective quartic Lagrangians are given by

$$i \frac{2\pi\alpha}{\cos^2\theta_W \Lambda^2} a_0 g_{\mu\nu} [g_{\alpha\beta}(p_1 \cdot p_2) - p_{2\alpha} p_{1\beta}], \quad (4)$$

$$\begin{aligned} & i \frac{\pi\alpha}{2\cos^2\theta_W \Lambda^2} a_c [(p_1 \cdot p_2)(g_{\mu\alpha} g_{\nu\beta} + g_{\mu\beta} g_{\alpha\nu}) + g_{\alpha\beta}(p_{1\mu} p_{2\nu} + p_{2\mu} p_{1\nu}) \\ & - p_{1\beta}(g_{\alpha\mu} p_{2\nu} + g_{\alpha\nu} p_{2\mu}) - p_{2\alpha}(g_{\beta\mu} p_{1\nu} + g_{\beta\nu} p_{1\mu})] \end{aligned} \quad (5)$$

where  $p_1$  and  $p_1$  are the momenta of photons.

The experimental bounds on the anomalous coupling parameters  $\frac{a_0}{\Lambda^2}$  and  $\frac{a_c}{\Lambda^2}$  are provided at the LEP through the process  $e^+e^- \rightarrow Z\gamma\gamma \rightarrow q\bar{q}\gamma\gamma$  by L3 collaboration, and from a combination of the processes  $e^+e^- \rightarrow Z\gamma\gamma \rightarrow q\bar{q}\gamma\gamma$  and  $e^+e^- \rightarrow Z\gamma\gamma \rightarrow \nu\bar{\nu}\gamma\gamma$  by OPAL collaboration. Recent results from L3 collaboration for quartic anomalous  $ZZ\gamma\gamma$  couplings are given by [3]

$$-0.02 \text{ GeV}^{-2} < \frac{a_0}{\Lambda^2} < 0.03 \text{ GeV}^{-2}, \quad (6)$$

$$-0.07 \text{ GeV}^{-2} < \frac{a_c}{\Lambda^2} < 0.05 \text{ GeV}^{-2}. \quad (7)$$

However, the current most restrictive experimental bounds are obtained by OPAL collaboration. These are

$$-0.007 \text{ GeV}^{-2} < \frac{a_0}{\Lambda^2} < 0.023 \text{ GeV}^{-2}, \quad (8)$$

$$-0.029 \text{ GeV}^{-2} < \frac{a_c}{\Lambda^2} < 0.029 \text{ GeV}^{-2}. \quad (9)$$

at 95% C. L. [4].

Up to now, the anomalous quartic  $ZZ\gamma\gamma$  couplings at the linear  $e^+e^-$  colliders and its  $e\gamma$  and  $\gamma\gamma$  options have been investigated via the processes  $e^+e^- \rightarrow Z\gamma\gamma$  [5, 6],  $e^+e^- \rightarrow ZZ\gamma$  [7],  $e^+e^- \rightarrow q\bar{q}\gamma\gamma$  [8],  $e\gamma \rightarrow ZZe$  [9],  $e\gamma \rightarrow Z\gamma e$  [10], and  $\gamma\gamma \rightarrow WWZ$  [11]. These vertices also have been examined at hadron colliders through the processes  $p\bar{p} \rightarrow Z\gamma\gamma$  [12],  $pp(\bar{p}) \rightarrow \gamma\gamma\ell\ell$  [13],  $pp \rightarrow p\gamma^*\gamma^*p \rightarrow pZZp$  [14–17],  $pp \rightarrow p\gamma^*p \rightarrow pZZqX$  [18],  $pp \rightarrow p\gamma^*p \rightarrow p\gamma ZqX$  [19],  $pp \rightarrow qq\gamma\ell\ell$  [20].

## II. EQUIVALENT PHOTON APPROXIMATION AT THE LINEAR COLLIDER

In the next few years, since the LHC has high center-of-mass energy and high luminosity, it is expected to answer some of the fundamental open questions in particle physics. However, the LHC may not procure high precision measurements as a result remnants of usual  $pp$  deep inelastic processes. For high precision measurements, a few TeV scale linear  $e^+e^-$

colliders which have extremely high luminosity and clean experimental environments must be built to complete the LHC. The most popularly envisaged linear collider is the Compact Linear Collider (CLIC) [21, 22]. The CLIC has been planned to carry out research into three different energy stages, and the basic parameters of these stages are given in Table I. The other well-known applications of linear colliders are to investigate new physics beyond the SM with the aid of  $e\gamma^*$  and  $\gamma^*\gamma^*$  reactions. An almost real  $\gamma^*$  photon emitted from either of the incoming leptons can interact with the other lepton soon after, and the process  $e^+e^- \rightarrow e^+\gamma^*e^- \rightarrow e^+ZZe^-$  can take place, as shown in Fig. 1. In addition, the photons emitted from both leptons collide with each other, and the process  $e^+e^- \rightarrow e^+\gamma^*\gamma^*e^- \rightarrow e^+ZZe^-$  can be produced, as given by Fig. 2. Almost real photons in these reactions have been defined by equivalent photon approximation (EPA) [23–25]. In this approximation, photons emitted from incoming leptons which have very low virtuality are scattered at very small angles from the beam pipe. Because the emitted almost real photons have a low virtuality, they are assumed to be on mass shell. Investigation of new physics beyond the SM through photon-induced reactions with EPA in the literature is not a very new phenomenon. Phenomenological searches contain: gauge boson self-interactions, excited neutrino, extradimensions, unparticle physics, supersymmetry, electromagnetic moments of the tau lepton, and so forth [26–47].

The fundamental aim of the current study is to investigate the physics potential of the CLIC via the reactions  $e^+e^- \rightarrow ZZ\gamma$ ,  $e^+e^- \rightarrow e^+\gamma^*e^- \rightarrow e^+ZZe^-$ , and  $e^+e^- \rightarrow e^+\gamma^*\gamma^*e^- \rightarrow e^+ZZe^-$  to examine anomalous quartic  $ZZ\gamma\gamma$  couplings.

### III. CROSS SECTIONS

Tree-level Feynman diagrams for the processes  $e^+e^- \rightarrow ZZ\gamma$ , and the subprocesses  $e^-\gamma^* \rightarrow ZZe^-$ ,  $\gamma^*\gamma^* \rightarrow ZZ$  are shown in Figs. 3-5. In the presence of the effective Lagrangians 2 and 3, the processes  $e^+e^- \rightarrow ZZ\gamma$  and the subprocesses  $e^-\gamma^* \rightarrow ZZe^-$  have only four Feynman diagrams. As shown in Figs. 3-4, while the first diagrams show the contribution coming from  $ZZ\gamma\gamma$  coupling, the other diagrams originate from SM electroweak processes. As seen from Fig. 5, the subprocess  $\gamma^*\gamma^* \rightarrow ZZ$  has only a Feynman diagram which consists of new physics. We have performed the  $ZZ\gamma\gamma$  vertex into the tree-level event generator, the COMPHEP-4.5.1, in order to study numerical calculations [48]. During our

work, only one of the anomalous coupling parameters  $\frac{a_0}{\Lambda^2}$  and  $\frac{a_c}{\Lambda^2}$  is presumed to deviate from the SM at any given time.

The total cross sections for the processes  $e^+e^- \rightarrow Z Z \gamma$ ,  $e^+e^- \rightarrow e^+\gamma^*e^- \rightarrow e^+Z Z e^-$  as functions of anomalous  $\frac{a_0}{\Lambda^2}$  and  $\frac{a_c}{\Lambda^2}$  couplings are plotted in Figs. 6-8. We understand from Figs. 6-8 that the value of the total cross section involving  $\frac{a_0}{\Lambda^2}$  coupling is greater than the value of the  $\frac{a_c}{\Lambda^2}$ . Hence, we anticipate that bound on the  $\frac{a_0}{\Lambda^2}$  parameter is obtained with a higher precision with respect to the bound on  $\frac{a_c}{\Lambda^2}$ .

#### IV. SENSITIVITY TO THE ANOMALOUS COUPLINGS

The SM events numbers for the processes  $e^+e^- \rightarrow Z Z \gamma$  and  $e^+e^- \rightarrow e^+\gamma^*e^- \rightarrow e^+Z Z e^-$  are given by

$$N_{SM} = L_{int} \times \sigma_{SM} \times BR(Z \rightarrow \ell\bar{\ell})^2 \quad (\ell = e, \mu) \quad (10)$$

where  $L_{int}$  is the integrated luminosity and  $\sigma_{SM}$  is the SM cross section. Here, we considered fully-leptonic decay channels of the final Z bosons of both processes the lepton channels of which are well-determined experimentally. Hence, the branching ratio of the Z boson pairs in the final states of both processes is  $BR(Z \rightarrow \ell\bar{\ell})^2 = 4.52 \times 10^{-3}$ . Therefore, the SM background cross sections for the processes  $e^+e^- \rightarrow Z Z \gamma$  and  $e^+e^- \rightarrow e^+\gamma^*e^- \rightarrow e^+Z Z e^-$  are given in Table II.

On the other hand, the SM cross section of the process  $e^+e^- \rightarrow e^+\gamma^*\gamma^*e^- \rightarrow e^+Z Z e^-$  is quite small, because the subprocess  $\gamma\gamma \rightarrow Z Z$  is not allowed at the tree level. It is only allowed at loop level and can be neglected [14–17]. Therefore, the observation of a few events at the end of such a process would be an important sign of new physics beyond the SM.

In our study, we use two different analyses for detailed research of the anomalous  $Z Z \gamma \gamma$  couplings. First, we employ a simple one-parameter  $\chi^2$  test when the number of SM events is greater than 10. This analysis only applies in the case of the process  $e^+e^- \rightarrow Z Z \gamma$  with center-of-mass energy of  $\sqrt{s} = 0.5$  TeV and integrated luminosity of  $230 \text{ fb}^{-1}$  since the SM event number is equal to 17. The  $\chi^2$  analysis is described as follows

$$\chi^2 = \left( \frac{\sigma_{SM} - \sigma_{NP}}{\sigma_{SM} \delta_{stat}} \right)^2 \quad (11)$$

where  $\sigma_{NP}$  is the total cross section in the presence of anomalous gauge couplings,  $\delta_{stat} = \frac{1}{\sqrt{N}}$  is the statistical error and here  $N$  is the number of events.

On the other hand, we carry out a Poisson distribution in the study of the anomalous couplings of all other processes due to the number of the SM events being fewer than 10. Sensitivity bounds are calculated by presuming the number of observed events to be equal to the SM prediction, i.e.,  $N_{obs} = L_{int} \times \sigma_{SM} \times BR(Z \rightarrow \ell\bar{\ell})^2$ . The upper limits of the number of events  $N_{up}$  at the 95% C.L. can be obtained as follows [15, 17]

$$\sum_{k=0}^{N_{obs}} P_{Poisson}(N_{up}; k) = 0.05. \quad (12)$$

The value of upper limits  $N_{up}$  can be determined with respect to the value of the number of observed events [49]. The number of observed events  $N_{obs}$  and corresponding values for upper limits  $N_{up}$  at 95% C.L. by using the Poisson distribution for the processes  $e^+e^- \rightarrow ZZ\gamma$  and  $e^+e^- \rightarrow e^+\gamma^*\gamma^*e^- \rightarrow e^+ZZe^-$  with different values of luminosity and center-of-mass energy are given in Tables III-IV. Here, the calculated values for  $N_{obs}$  are rounded to the nearest integer. For example, the number of observed events for the process  $e\gamma \rightarrow ZZe$  with  $\sqrt{s} = 1.5$  TeV is obtained as 0.1 and 0.3 for  $L_{int} = 100$  and  $200 \text{ fb}^{-1}$ , respectively. Both values of the number of observed events have been rounded to 0. In all of the energy and luminosity values, since the number of observed events for the process  $e^+e^- \rightarrow e^+\gamma^*\gamma^*e^- \rightarrow e^+ZZe^-$  is equal to 0, the values of upper limits is always to be 3. The upper bounds of the number of events  $N_{up}$  at the 95% C.L. can be transformed into the bounds of anomalous couplings  $\frac{a_0}{\Lambda^2}$  and  $\frac{a_c}{\Lambda^2}$ .

In Tables V-VII, we give the obtained one-dimensional bounds on anomalous couplings  $\frac{a_0}{\Lambda^2}$  and  $\frac{a_c}{\Lambda^2}$  at 95% C.L. for the processes  $e^+e^- \rightarrow ZZ\gamma$ ,  $e^+e^- \rightarrow e^+\gamma^*e^- \rightarrow e^+ZZe^-$ , and  $e^+e^- \rightarrow e^+\gamma^*\gamma^*e^- \rightarrow e^+ZZe^-$  with some values of integrated luminosity and center-of-mass energy. As can be seen in Tables V-VII, if the CLIC for three processes has collected with  $\sqrt{s} = 0.5$  TeV and  $L_{int} = 10 \text{ fb}^{-1}$  of data, the bounds on  $\frac{a_0}{\Lambda^2}$  would be  $[-3.24 \times 10^{-4}; 3.12 \times 10^{-4}] \text{ GeV}^{-2}$  for  $e^+e^- \rightarrow ZZ\gamma$ ,  $[-3.30 \times 10^{-4}; 3.29 \times 10^{-4}] \text{ GeV}^{-2}$  for  $e^+e^- \rightarrow e^+\gamma^*e^- \rightarrow e^+ZZe^-$ ,  $[-1.00 \times 10^{-4}; 1.00 \times 10^{-4}] \text{ GeV}^{-2}$  for  $e^+e^- \rightarrow e^+\gamma^*\gamma^*e^- \rightarrow e^+ZZe^-$  and  $\frac{a_c}{\Lambda^2}$  would be  $[-6.19 \times 10^{-4}; 5.70 \times 10^{-4}] \text{ GeV}^{-2}$  for  $e^+e^- \rightarrow ZZ\gamma$ ,  $[-1.10 \times 10^{-4}; 1.09 \times 10^{-3}] \text{ GeV}^{-2}$  for  $e^+e^- \rightarrow e^+\gamma^*e^- \rightarrow e^+ZZe^-$ ,  $[-3.41 \times 10^{-4}; 3.41 \times 10^{-4}] \text{ GeV}^{-2}$  for  $e^+e^- \rightarrow e^+\gamma^*\gamma^*e^- \rightarrow e^+ZZe^-$ . We can easily understand that these bounds are more restrictive

than the best limits obtained from OPAL collaboration. In addition, in the case of the CLIC runs maximum energy and luminosity, the bounds on  $\frac{a_0}{\Lambda^2}$  would be  $[-1.76 \times 10^{-8}; 1.75 \times 10^{-8}]$   $\text{GeV}^{-2}$  for  $e^+e^- \rightarrow ZZ\gamma$ ,  $[-1.18 \times 10^{-7}; 1.18 \times 10^{-7}]$   $\text{GeV}^{-2}$  for  $e^+e^- \rightarrow e^+\gamma^*e^- \rightarrow e^+ZZe^-$ ,  $[-4.79 \times 10^{-8}; 4.79 \times 10^{-8}]$   $\text{GeV}^{-2}$  for  $e^+e^- \rightarrow e^+\gamma^*\gamma^*e^- \rightarrow e^+ZZe^-$  and  $\frac{a_c}{\Lambda^2}$  would be  $[-3.06 \times 10^{-8}; 3.04 \times 10^{-8}]$   $\text{GeV}^{-2}$  for  $e^+e^- \rightarrow ZZ\gamma$ ,  $[-4.55 \times 10^{-7}; 4.51 \times 10^{-7}]$   $\text{GeV}^{-2}$  for  $e^+e^- \rightarrow e^+\gamma^*e^- \rightarrow e^+ZZe^-$ ,  $[-1.79 \times 10^{-7}; 1.79 \times 10^{-7}]$   $\text{GeV}^{-2}$  for  $e^+e^- \rightarrow e^+\gamma^*\gamma^*e^- \rightarrow e^+ZZe^-$ . Hence, the best bounds for  $\frac{a_0}{\Lambda^2}$  and  $\frac{a_c}{\Lambda^2}$  improve roughly the sensitivity bounds by up to a factor of  $10^5$   $\text{GeV}^{-2}$  and  $10^6$   $\text{GeV}^{-2}$  with respect to current experimental bounds, respectively. Principally, it can be seen from a comparison of Tables V-VII that the sensitivity to anomalous couplings rapidly increases when the center-of-mass energy and integrated luminosity of the processes increase.

## V. CONCLUSIONS

Since the linear  $e^+e^-$  colliders and its  $e\gamma^*$  and  $\gamma^*\gamma^*$  options have very clean experimental conditions and are mostly free from QCD backgrounds, the anomalous quartic gauge couplings with high precision measurements with reference to LHC can be obtained. However, the anomalous quartic gauge couplings  $\frac{a_0}{\Lambda^2}$  and  $\frac{a_c}{\Lambda^2}$  are described by dimension 6 effective quartic Lagrangian. We can understand that the total cross sections containing these couplings have a higher energy dependence than the usual SM processes. Therefore, having a high center-of-mass energy, the linear collider is extremely important for the determination of the anomalous quartic gauge couplings. For these reasons, we probe the processes  $e^+e^- \rightarrow ZZ\gamma$ ,  $e^+e^- \rightarrow e^+\gamma^*e^- \rightarrow e^+ZZe^-$ , and  $e^+e^- \rightarrow e^+\gamma^*\gamma^*e^- \rightarrow e^+ZZe^-$  with decaying leptonically of  $Z$  bosons at the CLIC in order to obtain the sensitivities to anomalous quartic gauge couplings. Best bounds on  $\frac{a_0}{\Lambda^2}$  and  $\frac{a_c}{\Lambda^2}$  couplings from three processes is obtained through the process  $e^+e^- \rightarrow ZZ\gamma$ , and they are at the order of  $10^{-8}$   $\text{GeV}^{-2}$ . It has been shown that the bounds on anomalous couplings improve up to approximately  $10^{-5}$   $\text{GeV}^{-2}$  times for  $\frac{a_0}{\Lambda^2}$  and up to  $10^{-6}$   $\text{GeV}^{-2}$  times for  $\frac{a_c}{\Lambda^2}$ . In addition, the  $e^+e^- \rightarrow e^+\gamma^*\gamma^*e^- \rightarrow e^+ZZe^-$  process, due to the number of SM events being negligibly small, provides us an opportunity to examine anomalous quartic couplings. As a result, the CLIC is a suitable platform for the probing of anomalous  $ZZ\gamma\gamma$  coupling in  $e^+e^- \rightarrow ZZ\gamma$  as well as  $e^+e^- \rightarrow e^+\gamma^*e^- \rightarrow e^+ZZe^-$  and  $e^+e^- \rightarrow e^+\gamma^*\gamma^*e^- \rightarrow e^+ZZe^-$  processes.

- 
- [1] G. Belanger and F. Boudjema Phys. Lett. B 288 201 (1992).
  - [2] G. Belanger and F. Boudjema Phys. Lett. B 288 210 (1992).
  - [3] L3 Collaboration, Phys. Lett. B 540 43-51 (2002).
  - [4] G. Abbiendi *et al.*, OPAL Collaboration, Phys. Rev. D 70 032005 (2004).
  - [5] W. J. Stirling and A. Werthenbach, Eur. Phys. J. C 14 103-110 (2000).
  - [6] A. Gutierrez-Rodriguez, C. G. Honorato, J. Montano, and M. A. Perez, Phys. Rev. D 89 034003 (2014).
  - [7] G. Belanger, F. Boudjema, Y. Kurihara, D. Perret-Gallix, and A. Semenov, Eur. Phys. J. C 13 283-293 (2000).
  - [8] G. Montagna, M. Moretti, O. Nicrosini, M. Osmo, F. Piccinini, Phys. Lett. B 515 197-205 (2001).
  - [9] O. J. P. Eboli, M. C. Gonzalez-Garcia and S. F. Novaes, Nucl. Phys. B 411 381 (1994).
  - [10] S. Atag and İ. Sahin, Phys. Rev. D 75 073003 (2007).
  - [11] O. J. P. Eboli, M. B. Magro, P. G. Mercadante, and S. F. Novaes, Phys. Rev. D 52 15-21 (1995).
  - [12] P.J. Dervan, A. Signer, W.J. Stirling, and A. Werthenbach, J. Phys. G 26 607-615 (2000).
  - [13] O. J. P. Eboli, M. C. Gonzalez-Garcia, and S. M. Lietti, S. F. Novaes Phys. Rev. D 63 075008 (2001).
  - [14] E. Chapon, C. Royon and O. Kepka, Phys. Rev. D 81 074003 (2010).
  - [15] T. Pierzchala and K. Piotrkowski, Nucl. Phys. Proc. Suppl. 179-180 257 (2008).
  - [16] R. S. Gupta, Phys. Rev. D 85 014006 (2012).
  - [17] J. de Favereau de Jeneret, V. Lemaitre, Y. Liu, S. Ovin, T. Pierzchala, K. Piotrkowski, X. Rouby, N. Schul, M. Vander Donckt, arXiv:0908.2020.
  - [18] A. Senol, arXiv:1311.1370.
  - [19] İ. Sahin and B. Sahin, Phys. Rev. D 86, 115001 (2012).
  - [20] O. J. P. Eboli, M. C. Gonzalez-Garcia, and S. M. Lietti, Phys. Rev. D 69 095005 (2004).
  - [21] D. Dannheim *et al.*, CLIC  $e^+e^-$  Linear Collider Studies, arXiv:1305.5766v1.
  - [22] D. Dannheim *et al.*, CLIC  $e^+e^-$  Linear Collider Studies, arXiv:1208.1402.
  - [23] V. M. Budnev, I. F. Ginzburg, G. V. Meledin and V. G. Serbo, Phys. Rep. 15, 181 (1975).



- [24] G. Baur et al., Phys. Rep. 364, 359 (2002).
- [25] K. Piotrkowski, Phys. Rev. D 63, 071502 (2001).
- [26] O. Kepka and C. Royon, Phys. Rev. D 78, 073005 (2008).
- [27] V.A. Khoze, A. D. Martin and M.G. Ryskin, Eur. Phys. J. C 23, 311 (2002).
- [28] S. M. Lietti, A. A. Natale, C. G. Roldao and R. Rosenfeld, Phys. Lett. B 497, 243 (2001).
- [29] S. Atag, S. C. İnan and İ. Sahin, Phys. Rev. D 80, 075009 (2009).
- [30] İ. Sahin and S. C. İnan, JHEP 09, 069 (2009).
- [31] İ. Şahin *et al.*, Phys.Rev. D 88 095016 (2013).
- [32] S. Atag, S. C. İnan and İ. Sahin, JHEP 09, 042 (2010).
- [33] S. C. İnan, Phys. Rev. D 81, 115002 (2010).
- [34] S. Atag and A. A. Billur, JHEP 11, 060 (2010).
- [35] M.G. Albrow, T.D. Coughlin and J.R. Forshaw, Prog. Part. Nucl. Phys. 65,149-184 (2010).
- [36] İ. Sahin, and A. A. Billur, Phys. Rev. D 83, 035011 (2011).
- [37] R. S. Gupta, Phys. Rev. D 85 014006 (2012).
- [38] I. Sahin, Phys. Rev. D 85 033002 (2012).
- [39] I. Sahin, and M. Koksalsal, JHEP 03 100 (2011).
- [40] M. Köksal and S. C. İnan, arXiv:1305.7096.
- [41] M. Köksal and S. C. İnan, AHEP Volume 2014, Article ID 315826, 8 pages (2014).
- [42] M. Köksal, arXiv:1402.2915.
- [43] M. Köksal, arXiv:1402.3112.
- [44] A. A. Billur and M. Koksalsal, Phys. Rev. D 89 037301 (2014).
- [45] A. A. Billur and M. Koksalsal, arXiv:1311.5326.
- [46] A. A. Billur, Europhys. Lett. 101 21001 (2013).
- [47] B. Sahin and A. A. Billur, Phys. Rev. D 86 074026 (2012).
- [48] A. Pukhov *et al.*, Report No. INP MSU 98-41/542; arXiv:hep-ph/9908288; arXiv:hep-ph/0412191.
- [49] K. Nakamura et al. (Particle Data Group), J. Phys. G 37, 075021 (2010).

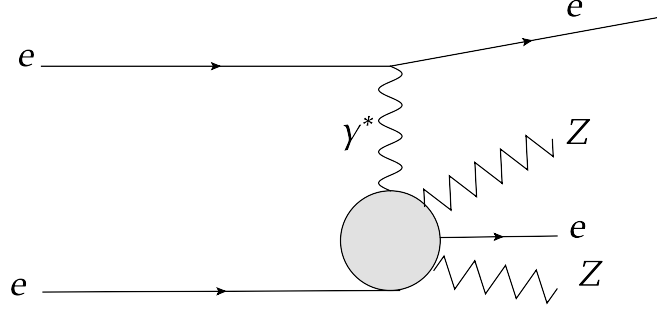


FIG. 1: Representative diagram for the process  $e^+e^- \rightarrow e^+\gamma^*e^- \rightarrow e^+ZZe^-$ .

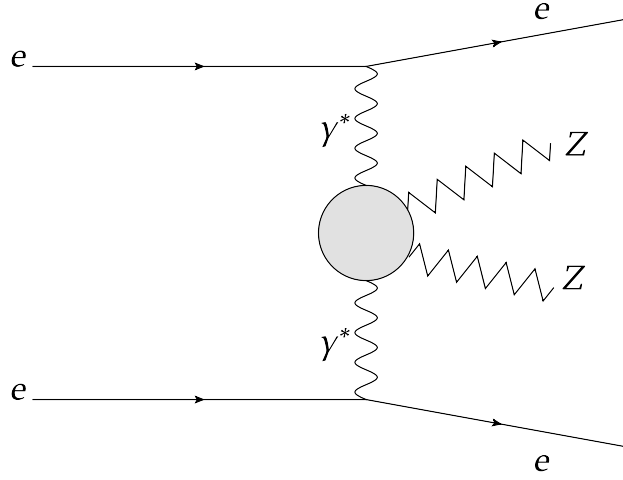


FIG. 2: Representative diagram for the process  $e^+e^- \rightarrow e^+\gamma^*\gamma^*e^- \rightarrow e^+ZZe^-$ .

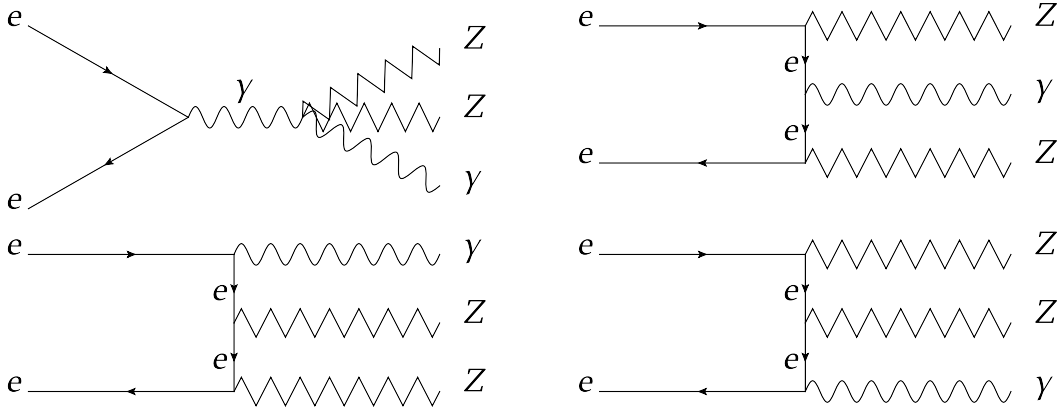


FIG. 3: Tree-level Feynman diagrams for the process  $e^+e^- \rightarrow ZZ\gamma$ .

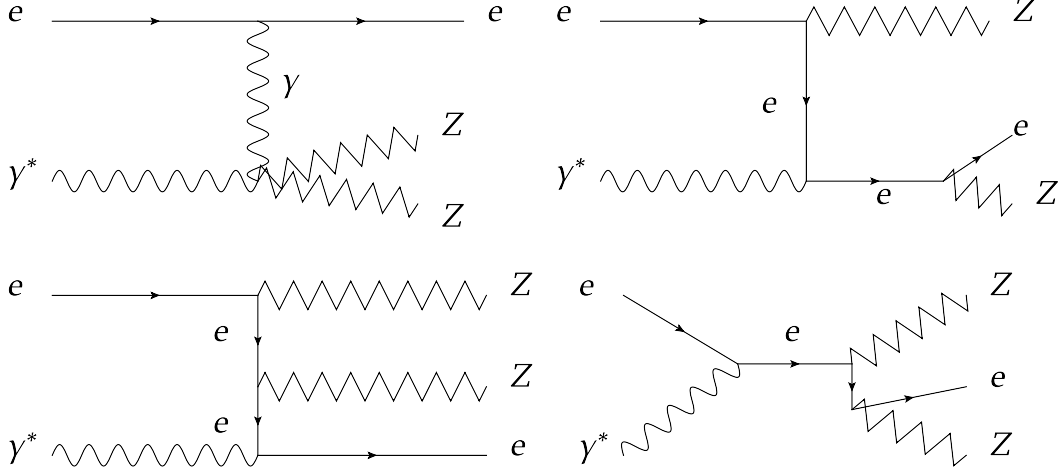


FIG. 4: Tree-level Feynman diagrams for the subprocess  $e^- \gamma^* \rightarrow Z Z e^-$ .

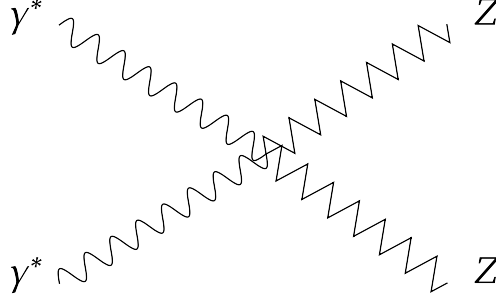


FIG. 5: Tree-level Feynman diagram for the subprocess  $\gamma^* \gamma^* \rightarrow Z Z$ .

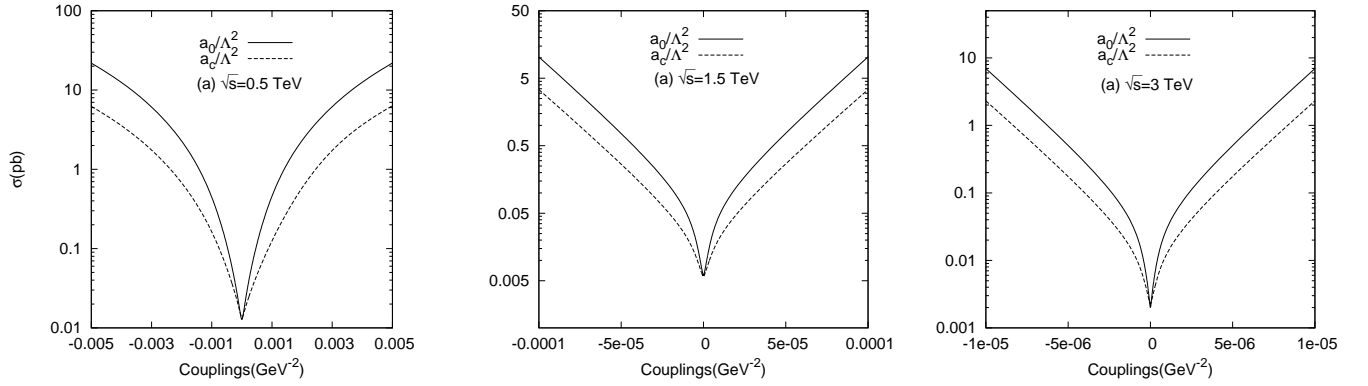


FIG. 6: The total cross sections as functions of anomalous  $\frac{a_0}{\Lambda^2}$  and  $\frac{a_c}{\Lambda^2}$  couplings for the process  $e^+ e^- \rightarrow Z Z \gamma$  at the CLIC with  $\sqrt{s} = 0.5, 1.5$  and  $3$  TeV.

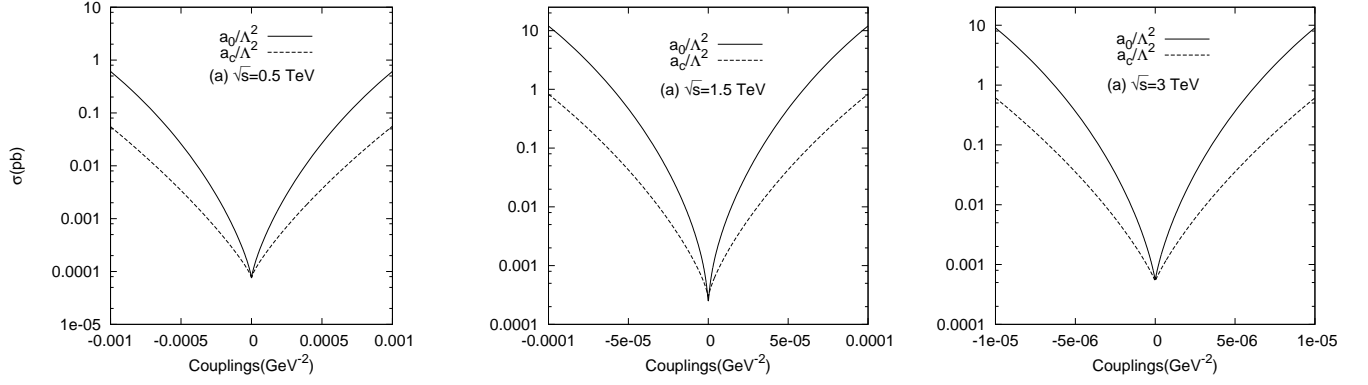


FIG. 7: The total cross sections as functions of anomalous  $\frac{a_0}{\Lambda^2}$  and  $\frac{a_c}{\Lambda^2}$  couplings for the process  $e^+e^- \rightarrow e^+\gamma^*e^- \rightarrow e^+ZZe^-$  at the CLIC with  $\sqrt{s} = 0.5, 1.5$  and 3 TeV.

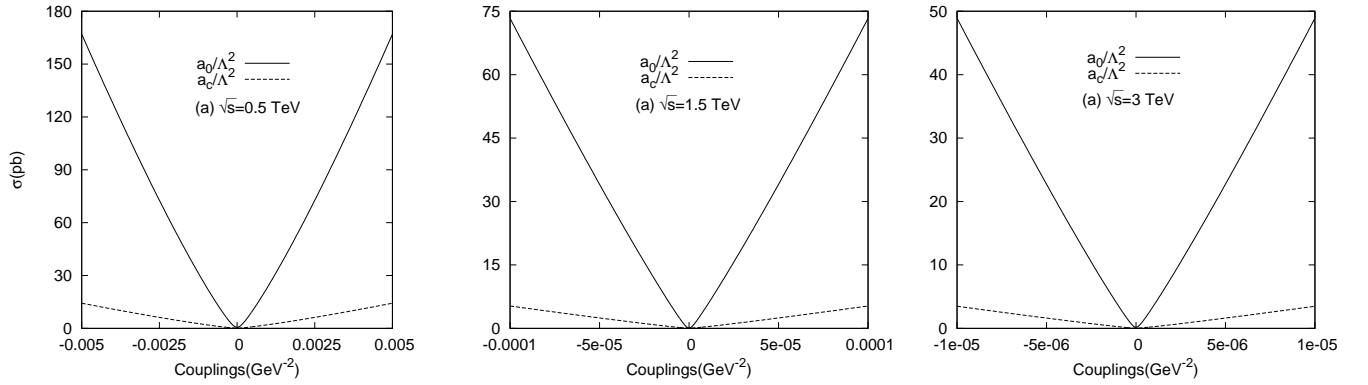


FIG. 8: The total cross sections as functions of anomalous  $\frac{a_0}{\Lambda^2}$  and  $\frac{a_c}{\Lambda^2}$  couplings for the process  $e^+e^- \rightarrow e^+\gamma^*\gamma^*e^- \rightarrow e^+ZZe^-$  at the CLIC with  $\sqrt{s} = 0.5, 1.5$  and 3 TeV.

TABLE I: The basic parameters of the three stages of the CLIC. Here  $\sqrt{s}$  is the center-of-mass energy,  $N$  is the number of particles in bunch,  $L$  is the total luminosity,  $\sigma_{x,y,z}$  are the average sizes of the bunches [22].

Parameter	Unit	Stage 1	Stage 2	Stage 3
$\sqrt{s}$	TeV	0.5	1.5	3
$N$	$10^9$	3.7	3.7	3.7
$L$	$\text{fb}^{-1}$	230	320	590
$\sigma_x$	nm	100	60	40
$\sigma_y$	nm	2.6	1.5	1
$\sigma_z$	$\mu\text{m}$	44	44	44

TABLE II: The SM background cross sections for the processes  $e^+e^- \rightarrow ZZ\gamma$  and  $e^+e^- \rightarrow e^+\gamma^*e^- \rightarrow e^+ZZe^-$  at the CLIC. Here, we impose the acceptance cuts on the pseudorapidities  $|\eta^{\ell,\gamma}| < 2.5$  and the transverse momenta  $p_T^\gamma > 20$  GeV,  $p_T^e > 25$  GeV for electron and photon in the final state of both processes.

Process	$\sqrt{s}$ (TeV)	SM Cross Section ( $\text{pb}^{-1}$ )
$e^+e^- \rightarrow ZZ\gamma$	0.5	$1.64 \times 10^{-2}$
	1.5	$5.69 \times 10^{-3}$
	3	$2.30 \times 10^{-3}$
$e^+e^- \rightarrow e^+\gamma^*e^- \rightarrow e^+ZZe^-$	0.5	$7.68 \times 10^{-5}$
	1.5	$3.59 \times 10^{-4}$
	3	$5.24 \times 10^{-4}$

TABLE III: The number of observed events  $N_{obs}$  and corresponding values for upper limits  $N_{up}$  at 95% C.L. for the process  $e^+e^- \rightarrow Z Z \gamma$  with different values of luminosity and center-of-mass energy.

$\sqrt{s}$ (TeV)	$L_{int}(\text{fb}^{-1})$	$N_{obs}$	$N_{up}$
0.5	10	1	4.74
0.5	50	4	9.15
0.5	100	7	13.15
1.5	10	0	3
1.5	100	3	7.75
1.5	200	5	10.51
1.5	320	8	14.43
3	10	0	3
3	100	1	4.74
3	300	3	7.75
3	590	6	11.84

TABLE IV: The number of observed events  $N_{obs}$  and associated values for upper limits  $N_{up}$  at 95% C.L. for the process  $e^+e^- \rightarrow e^+\gamma^*e^- \rightarrow e^+ZZe^-$  with different values of luminosity and center-of-mass energy.

$\sqrt{s}$ (TeV)	$L_{int}(\text{fb}^{-1})$	$N_{obs}$	$N_{up}$
0.5	10	0	3
0.5	50	0	3
0.5	100	0	3
0.5	230	0	3
1.5	10	0	3
1.5	100	0	3
1.5	200	0	3
1.5	320	1	4.74
3	10	0	3
3	100	0	3
3	300	1	4.74
3	590	1	4.74

TABLE V: The anomalous quartic gauge coupling parameters  $\frac{a_0}{\Lambda^2}$  and  $\frac{a_c}{\Lambda^2}$  at 95% C.L. for the process  $e^+e^- \rightarrow ZZ\gamma$  with various CLIC luminosities. The center of mass energies of the process are taken to be  $\sqrt{s} = 0.5, 1.5$  and 3 TeV.

$\sqrt{s}$ (TeV)	$L_{int}(\text{fb}^{-1})$	$\frac{a_0}{\Lambda^2}(\text{GeV}^{-2})$	$\frac{a_c}{\Lambda^2}(\text{GeV}^{-2})$
0.5	10	$[-3.24 \times 10^{-4}; 3.12 \times 10^{-4}]$	$[-6.19 \times 10^{-4}; 5.70 \times 10^{-4}]$
0.5	50	$[-1.72 \times 10^{-4}; 1.59 \times 10^{-4}]$	$[-3.34 \times 10^{-4}; 2.86 \times 10^{-4}]$
0.5	100	$[-1.27 \times 10^{-4}; 1.14 \times 10^{-4}]$	$[-2.53 \times 10^{-4}; 2.02 \times 10^{-4}]$
0.5	230	$[-1.01 \times 10^{-4}; 0.88 \times 10^{-4}]$	$[-2.01 \times 10^{-4}; 1.53 \times 10^{-4}]$
1.5	10	$[-7.68 \times 10^{-6}; 7.66 \times 10^{-6}]$	$[-1.35 \times 10^{-5}; 1.34 \times 10^{-5}]$
1.5	100	$[-3.34 \times 10^{-6}; 3.30 \times 10^{-6}]$	$[-5.87 \times 10^{-6}; 5.75 \times 10^{-6}]$
1.5	200	$[-2.41 \times 10^{-6}; 2.36 \times 10^{-6}]$	$[-4.24 \times 10^{-6}; 4.13 \times 10^{-6}]$
1.5	320	$[-2.06 \times 10^{-6}; 2.02 \times 10^{-6}]$	$[-3.61 \times 10^{-6}; 3.51 \times 10^{-6}]$
3	10	$[-9.61 \times 10^{-8}; 9.60 \times 10^{-8}]$	$[-1.67 \times 10^{-7}; 1.67 \times 10^{-7}]$
3	100	$[-3.56 \times 10^{-8}; 3.55 \times 10^{-8}]$	$[-6.17 \times 10^{-8}; 6.14 \times 10^{-8}]$
3	300	$[-2.22 \times 10^{-8}; 2.22 \times 10^{-8}]$	$[-3.86 \times 10^{-8}; 3.84 \times 10^{-8}]$
3	590	$[-1.76 \times 10^{-8}; 1.75 \times 10^{-8}]$	$[-3.06 \times 10^{-8}; 3.04 \times 10^{-8}]$



TABLE VI: The anomalous quartic gauge coupling parameters  $\frac{a_0}{\Lambda^2}$  and  $\frac{a_c}{\Lambda^2}$  at 95% C.L. for the process  $e^+e^- \rightarrow e^+\gamma^*e^- \rightarrow e^+ZZe^-$  with various CLIC luminosities. The center of mass energies of the process are taken to be  $\sqrt{s} = 0.5, 1.5$  and 3 TeV.

$\sqrt{s}$ (TeV)	$L_{int}(\text{fb}^{-1})$	$\frac{a_0}{\Lambda^2}(\text{GeV}^{-2})$	$\frac{a_c}{\Lambda^2}(\text{GeV}^{-2})$
0.5	10	$[-3.30 \times 10^{-4}; 3.29 \times 10^{-4}]$	$[-1.10 \times 10^{-3}; 1.09 \times 10^{-3}]$
0.5	50	$[-1.48 \times 10^{-4}; 1.47 \times 10^{-4}]$	$[-4.92 \times 10^{-4}; 4.87 \times 10^{-4}]$
0.5	100	$[-1.04 \times 10^{-4}; 1.03 \times 10^{-4}]$	$[-3.47 \times 10^{-4}; 3.40 \times 10^{-4}]$
0.5	230	$[-0.69 \times 10^{-4}; 0.68 \times 10^{-4}]$	$[-2.29 \times 10^{-4}; 2.22 \times 10^{-4}]$
1.5	10	$[-7.43 \times 10^{-6}; 7.43 \times 10^{-6}]$	$[-2.83 \times 10^{-5}; 2.83 \times 10^{-5}]$
1.5	100	$[-2.30 \times 10^{-6}; 2.29 \times 10^{-6}]$	$[-8.74 \times 10^{-6}; 8.70 \times 10^{-6}]$
1.5	200	$[-1.58 \times 10^{-6}; 1.57 \times 10^{-6}]$	$[-6.02 \times 10^{-6}; 5.96 \times 10^{-6}]$
1.5	320	$[-1.20 \times 10^{-6}; 1.19 \times 10^{-6}]$	$[-4.59 \times 10^{-6}; 4.54 \times 10^{-6}]$
3	10	$[-8.52 \times 10^{-7}; 8.52 \times 10^{-7}]$	$[-3.28 \times 10^{-6}; 3.28 \times 10^{-6}]$
3	100	$[-2.60 \times 10^{-7}; 2.60 \times 10^{-7}]$	$[-9.99 \times 10^{-7}; 9.97 \times 10^{-7}]$
3	300	$[-1.82 \times 10^{-7}; 1.82 \times 10^{-7}]$	$[-6.98 \times 10^{-7}; 6.96 \times 10^{-7}]$
3	590	$[-1.18 \times 10^{-7}; 1.18 \times 10^{-7}]$	$[-4.55 \times 10^{-7}; 4.51 \times 10^{-7}]$

TABLE VII: The anomalous quartic gauge coupling parameters  $\frac{a_0}{\Lambda^2}$  and  $\frac{a_c}{\Lambda^2}$  at 95% C.L. for the process  $e^+e^- \rightarrow e^+\gamma^*\gamma^*e^- \rightarrow e^+ZZe^-$  with various CLIC luminosities. The center of mass energies of the process are taken to be  $\sqrt{s} = 0.5, 1.5$  and 3 TeV.

$\sqrt{s}$ (TeV)	$L_{int}(\text{fb}^{-1})$	$\frac{a_0}{\Lambda^2}(\text{GeV}^{-2})$	$\frac{a_c}{\Lambda^2}(\text{GeV}^{-2})$
0.5	10	$[-1.00 \times 10^{-4}; 1.00 \times 10^{-4}]$	$[-3.41 \times 10^{-4}; 3.41 \times 10^{-4}]$
0.5	50	$[-0.45 \times 10^{-4}; 0.45 \times 10^{-4}]$	$[-1.52 \times 10^{-4}; 1.52 \times 10^{-4}]$
0.5	100	$[-0.32 \times 10^{-4}; 0.32 \times 10^{-4}]$	$[-1.08 \times 10^{-4}; 1.08 \times 10^{-4}]$
0.5	230	$[-0.21 \times 10^{-4}; 0.21 \times 10^{-4}]$	$[-0.71 \times 10^{-4}; 0.71 \times 10^{-4}]$
1.5	10	$[-3.01 \times 10^{-6}; 3.01 \times 10^{-6}]$	$[-1.12 \times 10^{-5}; 1.12 \times 10^{-5}]$
1.5	100	$[-9.51 \times 10^{-7}; 9.51 \times 10^{-7}]$	$[-3.54 \times 10^{-6}; 3.54 \times 10^{-6}]$
1.5	200	$[-6.73 \times 10^{-7}; 6.73 \times 10^{-7}]$	$[-2.51 \times 10^{-6}; 2.51 \times 10^{-6}]$
1.5	320	$[-5.32 \times 10^{-7}; 5.32 \times 10^{-7}]$	$[-1.98 \times 10^{-6}; 1.98 \times 10^{-6}]$
3	10	$[-3.68 \times 10^{-7}; 3.68 \times 10^{-7}]$	$[-1.38 \times 10^{-6}; 1.38 \times 10^{-6}]$
3	100	$[-1.17 \times 10^{-7}; 1.17 \times 10^{-7}]$	$[-4.36 \times 10^{-7}; 4.36 \times 10^{-7}]$
3	300	$[-6.72 \times 10^{-8}; 6.72 \times 10^{-8}]$	$[-2.52 \times 10^{-7}; 2.52 \times 10^{-7}]$
3	590	$[-4.79 \times 10^{-8}; 4.79 \times 10^{-8}]$	$[-1.79 \times 10^{-7}; 1.79 \times 10^{-7}]$